Pflugers Arch – Eur J Physiol (2006)
DOI 10.1007/s00424-005-1515-2

ION CHANNELS, TRANSPORTERS

Mark L. Chapman · Marie L. Blanke
Howard S. Krovetz · Antonius M.J. VanDongen

Allosteric effects of external K^+ ions mediated by the aspartate of the GYGD signature sequence in the Kv2.1 K^+ channel

Received: 5 April 2005 / Revised: 12 August 2005 / Accepted: 31 August 2005 / Published online: 10 November 2005

Abstract K^+ channels achieve exquisite ion selectivity without jeopardizing efficient permeation by employing multiple, interacting K^+-binding sites. Introduction of a cadmium (Cd^{2+})-binding site in the external vestibule of Kv2.1 (drk1), allowed us to functionally characterize a binding site for external monovalent cations. Permeant ions displayed higher affinity for this site than non-permeant monovalent cations, although the selectivity profile was different from that of the channel. Point mutations identified the highly conserved aspartate residue immediately following the selectivity filter as a critical determinant of the antagonism between external K^+ and Cd^{2+} ions. A conservative mutation at this position (D378E) significantly affected the open-state stability. Moreover, the mean open time was found to be modulated by external K^+ concentration, suggesting a coupling between channel closing and the permeation process. Reducing the Rb^+ conductance by mutating the selectivity filter to the sequence found in Kv4.1, also significantly reduced the effectiveness of Rb^+ ions to antagonize Cd^{2+} inhibition, thereby implicating the selectivity filter as the site at which K^+ ions exert their antagonistic effect on Cd^{2+} block. The equivalent of D378 in KcsA, D80, takes part in an inter-subunit hydrogen-bond network that allows D80 to functionally interact with the selectivity filter. The results suggest that external K^+ ions antagonize Cd^{2+} inhibition (in I379C) and modulate the mean open time (in the wild-type Kv2.1) by altering the occupancy profile of the K^+-binding sites in the selectivity filter.

M. L. Chapman · M. L. Blanke · H. S. Krovetz
A. M. J. VanDongen (✉)
Department of Pharmacology, Duke University,
Durham, NC, USA
E-mail: vando005@mc.duke.edu
Tel.: +1-919-6814862

Introduction

Permeation and gating are two fundamental aspects of ion-channel function. Since Hodgkin and Huxley's quantitative description of voltage-dependent conductances in squid giant axon [1], permeation and gating have been considered distinct, independent components of ion-channel behavior. Molecular cloning of voltage-gated channels and subsequent mutagenesis experiments further strengthened this idea, by assigning separate structural elements to the activation machinery and the permeation pathway. Voltage-gated K^+ channels consist of four identical subunits, symmetrically assembled around a central aqueous pore, each containing hydrophobic domains (S1–S6). The fourth transmembrane segment (S4) was identified as a critical element of the voltage sensor [2–7], while the structure forming the permeation pathway was localized to the P-region between S5 and S6 [8–12]. Experiments employing macroscopic *Shaker* K^+ currents suggested that the C-terminal part of S6 forms the gate [13–15]. The crystallographic structure of the bacterial KcsA K^+ channel [16] indeed contains a narrow cytoplasmic constriction formed by the TM2 segments, supporting the idea of a cytoplasmic gate [17]. Additional support came from EPR spectroscopy measurements in KcsA, which revealed rotational movements of TM2 following activation, and a subsequent widening of the cytoplasmic constriction [18, 19]. A structural model for the open channel was obtained when the calcium-activated MthK K^+ channel was crystallized in the Ca^{2+}-bound, opened state [20].

Although gating and permeation properties are determined by two structures at opposite ends of the pore, these processes appear to be strongly coupled as indicated by the ability of the permeant ions to modulate gating parameters, including activation, deactivation, inactivation, open probability and open time [21–32]. In Kv2.1, external K^+ ions binding to a site in the selectivity filter determine the conformation of the external

vestibule [33] and thereby affect the affinity and efficacy of tetraethylammonium (TEA) [34, 35] inactivation rate [36, 37] and the macroscopic K^+ conductance [38]. A strict coupling between gating and permeation has also been proposed to explain subconductance behavior in single-channel recordings [39, 40]. Subconductance levels are more abundant when channels are partially activated [41–43], linking them to the activation pathway. In many channels, sublevels are preferentially observed during the transitions between the open and closed states [44, 45], directly associating them with the movement of the gate. Further evidence for the coupling between single channel gating and the permeation process came from the observation that subconductance levels display a different ion selectivity than the main open state [46] and from the cyclic, asymmetric gating between different conductance levels reported for the NMDA receptor [45]. Finally, backbone mutations in the selectivity filter have directly implicated this permeation structure in single-channel gating [47].

We have previously shown for Kv2.1 that cysteine substitution at I379C introduces a Cd^{2+}-binding site in the external vestibule. We now report that external K^+ ions antagonize this Cd^{2+} inhibition. The following results were obtained: (1) Cd^{2+} ions inhibit K^+-channel function through an allosteric mechanism; (2) mutation D378E in the GYGD signature sequence has two effects—it removes the K^+–Cd^{2+} antagonism and reduces open-state stability; (3) external K^+ ions also have dual effects: they antagonize the Cd^{2+} inhibition and modulate open-state stability; and (4) a mutation in the selectivity filter region that alters the ion selectivity of the channel also changes the selectivity profile of the antagonism of Cd^{2+} inhibition. It is concluded that external K^+ ions exert their effect by binding to sites in the filter. Analysis of the KcsA structure revealed an inter-subunit hydrogen-bond (H-bond) network that may allow D378 to monitor the occupancy profile of the selectivity filter. A model is proposed in which D378 mediates the allosteric coupling between external K^+ ions and Cd^{2+} ions.

Materials and methods

Molecular biology

Mutagenesis was performed using polymerase chain reaction (PCR) and Kv2.1 in the pBluescript plasmid vector. Oligonucleotides were designed using the OLIGO software (National Biosciences, Inc., Plymouth, MN). Mutagenesis of small restriction fragments was performed by the "Megaprimer" technique [48]. Mutated fragments were sequenced using a 7-deaza-GTP DNA Sequencing Kit (Amersham Biosciences, Piscataway, NJ). Plasmid DNA was linearized using the *Not*I restriction enzyme. Sense RNA was transcribed using T7 RNA polymerase. RNA was capped using m7G(5′)ppp(5′)G.

Electrophysiology

Oocyte preparation and cRNA injection were done as previously described [49]. Defolliculated oocytes were placed in a recording chamber perfused with one of the following solutions (concentrations in mM). Divalent-free solution: 100 LiCl, 10 HEPES; high-K solution: 100 KCl, 1 $MgCl_2$, 10 HEPES; high-Rb solution: 100 RbCl, 1 $MgCl_2$, 10 HEPES; low-K solution: 100 NaCl, 2 KCl, 1 $MgCl_2$, high-Na solution: 100 NaCl, 1 $MgCl_2$, 10 HEPES; monovalent solution: 200 sucrose, 1 $MgCl_2$, 10 mM of either LiCl, NaCl, RbCl or KCl. The pH was adjusted to 7.40 using NaOH for all solutions. K^+ current were recorded using a commercial two-electrode voltage clamp amplifier (Warner Instruments, Hamden, CT). Oocytes were impaled with two electrodes filled with 3 M KCl. The resistances of the current and voltage electrodes were 0.3–1.5 and 1.0–4.0 MΩ, respectively. Voltage-pulse protocols and data acquisition were managed by PClamp hardware and software (Axon Instruments, Burlingame CA). Linear leak and capacitive currents were corrected using a P/4 protocol. Inhibition by Cd^{2+} was evaluated using step depolarizations to +40 mV from a holding potential of −80 mV. Oocytes were perfused continuously with one of the above solutions, to which $CdCl_2$ was added to obtain the desired concentration. Single- channel currents were recorded from cell-attached patches on manually devitellinized oocytes. Patch pipettes were fabricated from thin-wall borosilicate (type 7740) capillaries (TW150F, WPI, Sarasota, FL), Sylgard (Dow-Corning Corp., Midland, MI) coated and fire polished. Solutions were as follows (concentrations in mM). Bath: 100 KCl, 60 KOH, 10 EGTA, 10 HEPES, 2 $MgCl_2$, pH 7.2 (HCl); pipette solution (1): (10 mM external KCl) = 150 NMDG, 5 KCl, 5 KOH, 2 $MgCl_2$, 2 $CaCl_2$, 10 HEPES, pH 7.20 (HCl); Pipette solution (2): (isotonic 160 KCl) = 155 KCl, 5 KOH, 2 $MgCl_2$, 2 $CaCl_2$, 10 HEPES, pH 7.20 (HCl). Data were acquired with an Axopatch 200 patch-clamp amplifier, Digidata 1200 interface and PClamp6 software (Axon Instruments). Currents were filtered at 1.5 kHz (−3 db, 4-pole Bessel filter), digitized at 5–10 kHz and stored on the computer hard disk for offline analysis. Linear leakage and capacitative currents were corrected using a smoothed average of empty traces. Idealization and analysis of single-channel recordings were performed with the Transit algorithm and software package [50].

Oocyte procurement

Xenopus laevis oocytes were harvested from adult female frogs using aseptic techniques. A female *X. laevis* is anesthetized in distilled water containing tricaine (0.75 g/l). A small (1 cm) incision is made through the skin and peritoneum, in the lower abdomen on the ventral side. A few ovarian lobes containing several hundred oocytes are removed. The incision is sutured

with two stitches in the peritoneum and two stitches in the skin. The frog is held in a recovery tank and monitored for 2 h.

Results

Cysteine-substitution of isoleucine 379 immediately following the GYGD signature sequence of the Kv2.1 (drk1) K^+ channel results in the introduction of a high-affinity soft-metal-binding site [51]. External Cd^{2+} ions inhibit outward K^+ currents in this I379C mutant channel in a concentration-dependent manner. Interestingly, the apparent affinity of I379C for Cd^{2+} ions was found to depend critically on the ionic composition of the external solution. We further explored this finding when it became clear that Cd^{2+} ions were interacting with external monovalent cations.

Antagonism of Cd^{2+} inhibition in I379C by external permeant ions

The Cd^{2+} affinity of I379C was originally determined in a divalent-free LiCl solution [51]. When these experiments were repeated in more physiological solutions, the Cd^{2+}-sensitivity of I379C was found to be substantially reduced. Adding 2 mM $MgCl_2$ to the divalent-free solution did not affect the Cd^{2+}-sensitivity (data not shown). Since the Cl^- concentration was the same for these experiments, the antagonism of Cd^{2+} inhibition had to result from a monovalent cation. To investigate this further, 10 mM of each of five monovalent cations (Li^+, Na^+, NH_4^+, K^+ and Rb^+) was added to a solution containing 200 mM sucrose, 2 mM $MgCl_2$ and 10 mM HEPES. Figure 1 illustrates the effect of the presence of 10 mM of various monovalent cations on Cd^{2+} inhibition. When the external solution contained the non-permeant ions Li^+ or Na^+, a substantial Cd^{2+} inhibition of the outward K^+ current was observed. However, in the presence of the permeant cation Rb^+ only a slight diminution of the outward current was apparent, while no inhibition was observed at all in the K^+-containing solution. Antagonism of Cd^{2+} inhibition by ammonium (NH_4^+) ions was intermediate between that of Na^+ and K^+ ions, although the permeability for NH_4^+ ions was very poor in Kv2.1. Therefore, monovalent cations antagonize Cd^{2+} inhibition of outward K^+ currents in Kv2.1-I379C with a selectivity profile ($K^+ > Rb^+ \gg NH_4^+ \gg Na^+ > - \gg Na^+ > Li^+$) that is distinct from the selectivity of the channel itself ($Rb^+ = K^+$; NH_4^+, Na^+ and Li^+ are virtually impermeant).

Concentration-dependence of the K^+ effect

Cd^{2+} inhibition was antagonized by external K^+ ions in a concentration-dependent manner (Fig. 1c). The antagonism of inhibition saturated with higher K^+ concentrations and the concentration-dependence was well described by the Hill equation (Fig. 1c). The Hill coefficient of 1.3 suggests that the effect of external K^+ ions on Cd^{2+} inhibition is mediated by more than one K^+-binding site. Whereas K^+ and Rb^+ ions antagonize current inhibition by Cd^{2+} when replacing Na^+ ions, substitution of Li^+ or $NMDG^+$ for Na^+ actually enhanced the effect of Cd^{2+} (data not shown). Therefore, it appears that permeant ions have a higher affinity for the K^+-binding site than non-permeant ions. Interestingly, this site is able to discriminate between non-permeating ions, since it binds Na^+ ions with higher affinity than Li^+ ions (Fig. 1a, b). These results indicate that introduction of a Cd^{2+}-binding site by the mutation I379C allows us to functionally characterize the properties of a set of external binding sites for monovalent cations. The binding sites display a unique selectivity profile and occupancy of these sites by permeant monovalent cations decreases the inhibition induced by Cd^{2+} ions in Kv2.1-I379C.

Cd^{2+} efficacy depends on the Debye length

The effect that external K^+ ions exert on Cd^{2+} inhibition could be due to either a direct competition of K^+ and Cd^{2+} ions for the same binding site, or it could involve an allosteric interaction between distinct sites. If the two ions bind to separate sites and interact through electrostatic repulsion, then increasing the Debye length of the external solution (by decreasing the ionic strength) will strengthen their interaction and K^+ ions should be more effective in displacing the Cd^{2+} ions. If, on the other hand, K^+ ions are directly competing for the Cd^{2+}-binding site formed by the thiols at position 379, then increasing the Debye length should increase the affinity of both cations. However, the effect should be stronger for the divalent Cd^{2+} and therefore the relative effectiveness of K^+ ions should decrease. Figure 2a illustrates that increasing the Debye length for a fixed concentration of both Cd^{2+} and K^+ ions results in a reduction of the efficacy with which Cd^{2+} ions inhibit K^+ currents. There are at least two explanations for this effect of ionic strength. It is conceivable that lowering the ionic strength alters the structure of the external vestibule and thereby it reduces the inhibitory effect that bound Cd^{2+} ions exert on the K^+ channel function. If, on the other hand, ionic strength does not affect the structure of the external vestibule, then the data are incompatible with K^+ ions and Cd^{2+} ions sharing the same binding site.

Voltage-dependence of the K^+ and Cd^{2+} effects

Both the accessibility of the K^+-binding site to the external environment and the electrostatic interaction with Cd^{2+} ions bound at I379C suggested that the sites were located in or near the external entrance of the

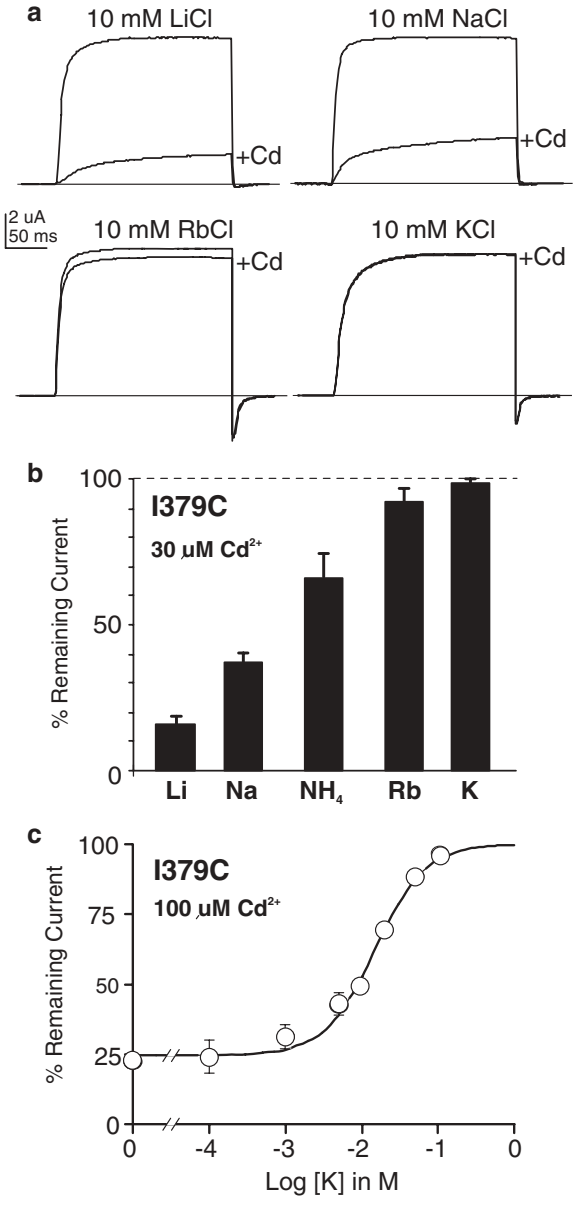

◀

Fig. 1 Ion-selectivity profile of the antagonism of Cd^{2+} inhibition. **a** Representative whole-cell current traces of the Kv2.1 (drk1) I379C mutant in five different external solutions: 200 mM sucrose to which was added 10 mM Na^+, Li^+, NH_4^+, Rb^+ or K^+ ions. For each recording condition, two representative traces show the current in the absence and in the presence of 30 μM Cd^{2+}. Outward K^+ currents were elicited by a 300-ms step depolarization to +40 mV from a holding potential of −80 mV. **b** Average inhibition by 30 μM Cd^{2+} of the I379C mutant in the same external solutions as shown in panel (**a**). Each average is calculated from a minimum of three oocytes. **c** Currents were elicited by a 300 ms step depolarization to +40 mV from a holding potential of -80 mV. Outward K^+ currents before and after the addition of 100 μM Cd^{2+} were determined and the percent of remaining current calculated. The external solution contained 100 mM LiCl with equimolar amounts of KCl (0, 1, 2, 5, 10, 20, 50 and 100 mM) substituted for LiCl. All points represent a minimum of four recordings. The concentration–response curve was fitted with the following Hill equation: $I_{Cd}/I_{control} = (1-I_0)/(1+((EC_{50}/[K^+])^n))$, where n is the Hill coefficient and I_0 the zero-K^+ asymptote. Parameter optimization was performed using Microsoft Excel with the XLFit version 4 add-in (ID Business solutions Ltd, Surrey, UK). Fitted values (mean ± SEM) for the potassium EC_{50} and Hill coefficient were: $EC_{50} = 13.9 \pm 1.4$ mM, $n = 1.3 \pm 0.1$

channel. This hypothesis was tested by determining the voltage-dependence of both Cd^{2+} inhibition and its antagonism by external K^+ ions (Fig. 2b). There was no significant difference in inhibition of outward currents between +20 and +60 mV, indicating a complete lack of voltage-dependence of Cd^{2+} binding. The ability of 10 mM external K^+ to antagonize Cd^{2+} inhibition, displayed a shallow voltage-dependence (Fig. 2b). The weak voltage-dependence may reflect that bound K^+ ions experience 7% of the membrane electric field. Alternatively, the K^+-binding site itself may be outside the membrane electric field, with its voltage-dependence resulting from a coupling to K^+ ions moving through the selectivity filter, as has been described for TEA [52, 53]. The K^+-binding sites outside the selectivity filter (S0 and S0′) would display such a behavior, because they are expected to be outside the membrane electric field, but their occupancy is strongly coupled to the sites S1–S4 in the filter [75]. Either way, the difference in the voltage-dependence further supports the idea that K^+ and Cd^{2+} ions bind to distinct sites.

Allosteric interaction or direct competition?

The difference in voltage-dependence and the effect of changing the Debye length on the interaction between K^+ and Cd^{2+} ions suggested that they bind at distinct sites. Therefore, the binding of Cd^{2+} in the presence of K^+ should be appropriately described by a model for allosteric competitive antagonism [54]. The model employs a coupling constant (α) that measures the strength of the allosteric interaction. The Ehlert allosteric antagonism model is an extension of the classical competitive antagonism model [55] allowing competitive interactions between molecules binding to two distinct sites. External K^+ concentration–response data in the presence of four Cd^{2+} concentrations were fitted individually with the allosteric antagonism model (Fig. 3). This resulted in estimates for the equilibrium dissociation constant (K_D) for K^+ ions, as well as its Hill coefficient (Table 1). Hill coefficients were greater than 1 for all four Cd^{2+} concentrations, suggesting multiple binding sites for external K^+ ions. The entire dataset was also simultaneously fitted with a single allosteric antagonism model, which resulted in a reduced goodness-of-fit (Fig. 3). The main problem is that the Hill coefficient for K^+ ions is too small to correctly describe the relatively steep curves. The coupling constant α was fairly large, indicating a strong interaction between K^+ and Cd^{2+} ions (Table 1).

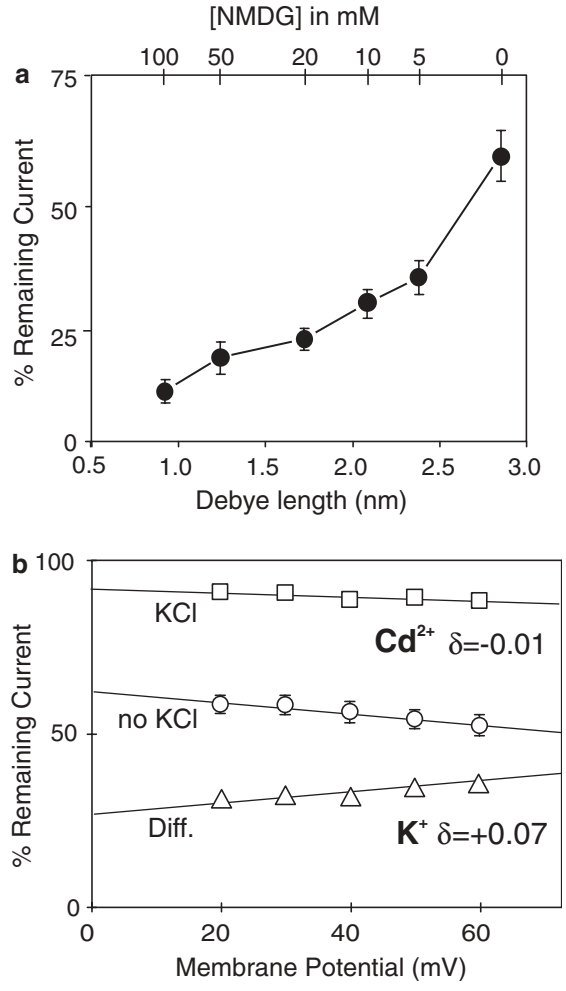

Fig. 2 Characterization of the K^+-binding site. **a** The nature of the interaction between K^+ and Cd^{2+} ions was investigated by varying the Debye length of the external solution. Outward K^+ currents were determined before and after the addition of 100 μM Cd^{2+} to the external solution, with the following composition: 200 mM sucrose, 10 mM HEPES, 1 mM $MgCl_2$ and 10 mM KCl. To vary the ionic strength, NMDG-Cl (0, 10, 20, 50 and 100 mM) was substituted iso-osmotically for sucrose. Currents were elicited by a 300-ms step depolarization to +40 mV from a holding potential of −80 mV. The percentage of current remaining after Cd^{2+} inhibition is plotted against the Debye length. **b** The voltage-dependence of Cd^{2+} and K^+ binding was determined for I379C by assessing Cd^{2+} inhibition (30 μM) in the presence and absence of external K^+ ions at five positive membrane potentials. The external solution was 100 mM NaCl, or the same solution with equimolar substitution of 10 mM KCl. All points represent a minimum of four recordings. The voltage-dependence of K^+ binding was evaluated by subtracting the Cd^{2+} inhibition values in the absence of K^+ ions from those in the presence of K^+ ions. The data were fitted with the Woodhull model to estimate δ, the fraction of the membrane potential experienced by Cd^{2+} and K^+ ions bound to their respective sites [76]

D378 is critical for K^+ ion antagonism of the Cd^{2+} block

In order to determine which amino acid(s) in the Kv2.1 K^+ channel play a critical role in the effect of external K^+ ions on Cd^{2+} inhibition, a series of point mutations was made at positions 376 to 380 in conjunction with the I379C mutation that introduces the soft- metal-binding site. The effect of the additional mutations was then tested by comparing Cd^{2+} IC_{50} s in external solutions containing either 100 mM Na^+ or 100 mM K^+ (Fig. 4, Table 2). Three of the four constructs yielded functional channels, all of which retained high-affinity Cd^{2+} binding. Moreover, all of the channels, except for one, also retained the K^+-dependent antagonism of Cd^{2+} binding. The lone exception was the conservative substitution of aspartate for glutamate in the GYGD signature sequence (D378E), in which the K^+ antagonism of Cd^{2+} binding was completely abrogated (Fig. 4, Table 2). Interestingly, the Cd^{2+} sensitivity was significantly increased by the D378E mutation (Fig. 4).

Mutation D378E decreases the open-state stability

The functional consequences of mutating aspartate 378 to glutamate (D378E) were further studied at the single-channel level. The single-channel behavior of D378E was markedly different from that of Kv2.1 (Fig. 5). The single-channel current was only slightly reduced in D378E. The primary effect of the mutation, however, was a destabilization of the open state. D378E open times were eight-fold shorter and openings were much more likely to occur in isolation, separated by long periods with no activity. Single-channel current–voltage relationships determined in isotonic 160 mM K^+ were linear over the voltage range studied (Fig. 5c). Slope conductances were not significantly different from each other. In contrast to the limited effect on single-channel conductance, the mean open time was significantly reduced by D378E (Fig. 5d).

Effect of external K^+ ions on single-channel gating

Mutation of aspartate 378 to glutamate (D378E) had two significant consequences: (1) it eliminated the ability of external K^+ ions to antagonize Cd^{2+} inhibition in I379C and (2) it produced pronounced effects on single-channel gating, destabilizing the open state and reducing the open probability. This suggested that there may be a relationship between external K^+ ions and single-channel gating. Therefore, the effects of external K^+ ions on single-channel behavior were further explored. The mean open time was found to depend on external K^+ concentrations for both Kv2.1 and D378E (Fig. 6a), increasing 2.2- and 2.5-fold between 1 and 100 mM external K^+ for Kv2.1 and D378E, respectively. This K^+-dependence could be reasonably well described by the Hill equation. The D378E mutation increased the K^+ EC_{50} and severely shifted the range over which K^+ ions can modulate the mean open time. The single-channel conductance also depended on external K^+

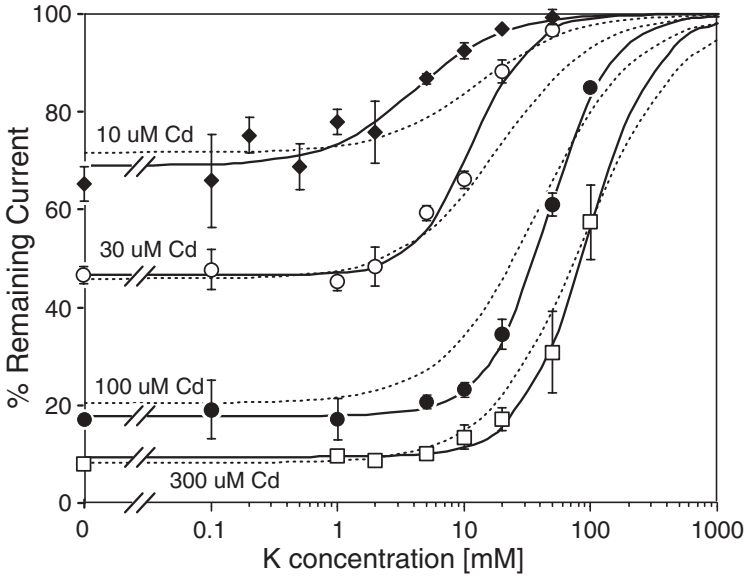

Fig. 3 Allosteric vs competitive antagonism. The antagonism between external K^+ and Cd^{2+} ions seen in I379C could result from competition for the same binding site [55]. Alternatively, if K^+ and Cd^{2+} ions bind to unique sites, but interfere with each others binding through electrostatic repulsion, then the more general model by Ehlert (1988) for allosteric competitive antagonism [54] would be more suitable. This model reverts to the Gaddum model when the coupling coefficient ,α (*vide infra*) becomes very large. We have amended the allosteric model to incorporate Hill coefficients for both K^+ and Cd^{2+}. In this model, the fraction of K^+ current remaining (F) following Cd^{2+} block is: $F = 1 - \frac{1}{1+\left(K'_{Cd}/[Cd]\right)^{n_{Cd}}}$ with $K_{Cd} = \frac{(K_K/[K])^{n_K}+1}{(K_K/[K])^{n_K}+1/\alpha}$ where K_{Cd} and K_K are the equilibrium dissociation constants for Cd^{2+} and K^+, respectively, n_{Cd} and n_K are the respective Hill coefficients and α is the coupling factor. The fraction of the remaining current was determined after switching the perfusion to a solution containing 10, 30, 100 or 300 μM Cd^{2+}. The external solution was 100 mM NaCl, 2 mM $MgCl_2$ (pH 7.4) with equimolar amounts of KCl substituted for NaCl. The results of fitting each of the four K^+-concentration–response curves individually with the Ehlert model are illustrated. The Cd^{2+} affinity constant and its Hill coefficient were determined previously [51] and these parameters were fixed at their known values ($K_{Cd} = 24$ μM; $n_{Cd} = 1.2$). *Dotted lines* show the results of fitting the entire dataset with a single model. Optimized parameters (K_D and Hill coefficient for K^+ ions and coupling coefficient α are provided in Table 1. The curves were also individually fitted with the Hill equation (data not shown), resulting in the following estimates for the Hill coefficient (mean ± SEM): 1.0 ± 0.3, 1.9 ± 0.3, 1.7 ± 0.1 and 1.7 ± 0.1 for 10, 30, 100 and 300 μM Cd^{2+}, respectively. The last three values are significantly greater than 1.0 ($P < 0.02$)

concentration. The D378E mutation resulted in a small reduction of the single-channel conductance for all K^+ concentrations (Fig. 6b).

Possible locations for the K^+-binding sites

The amino acid sequence of the pore region of voltage-gated K^+ channels is highly conserved with that of the prokaryotic K^+ channels KcsA [56, 57], MthK [20], KvAP and BirBac [58], for which high-resolution X-ray structures are available. This suggests that the available X-ray structures provide a reasonable structural model for the pore of Kv2.1. All the crystallized K^+ channels contain a selectivity filter, whose structure is remarkably conserved. There are five positions in the selectivity filter (S0–S4) at which K^+ ions are preferentially found. The most external of these positions are obvious candidates for the K^+-binding sites that are functionally characterized here. However, there are other possible sites which could be responsible for the effect of external K^+ ions. D378 in Kv2.1 corresponds to D80 in KcsA, which is not part of the selectivity filter, but rather points away from it. Analysis of the local environment of D80 in the KcsA structure revealed that D80, together with five of its nearest neighbors, forms a cavity flanked by the selectivity filter and the pore helix. The cavities are highly electronegative, providing an environment suitable for water molecules and, possibly, cations. Molecular dynamics simulations have suggested that water molecules indeed fill these small cavities, where they affect the conformational dynamics of the filter [59]. A functional K^+ channel contains four equivalent cavities/pockets symmetrically arranged around

Table 1 Fitted parameters for allosteric model shown in Fig. 3. Potassium affinity constant (K_D K) in mM

Cd concentrations	10	30	100	300	All four
K_D K	5.1	9.6	25.9	22.8	14.9
Hill K	2.24	2.42	2.25	1.65	1.33
α	25	87	89	42,227	1,647

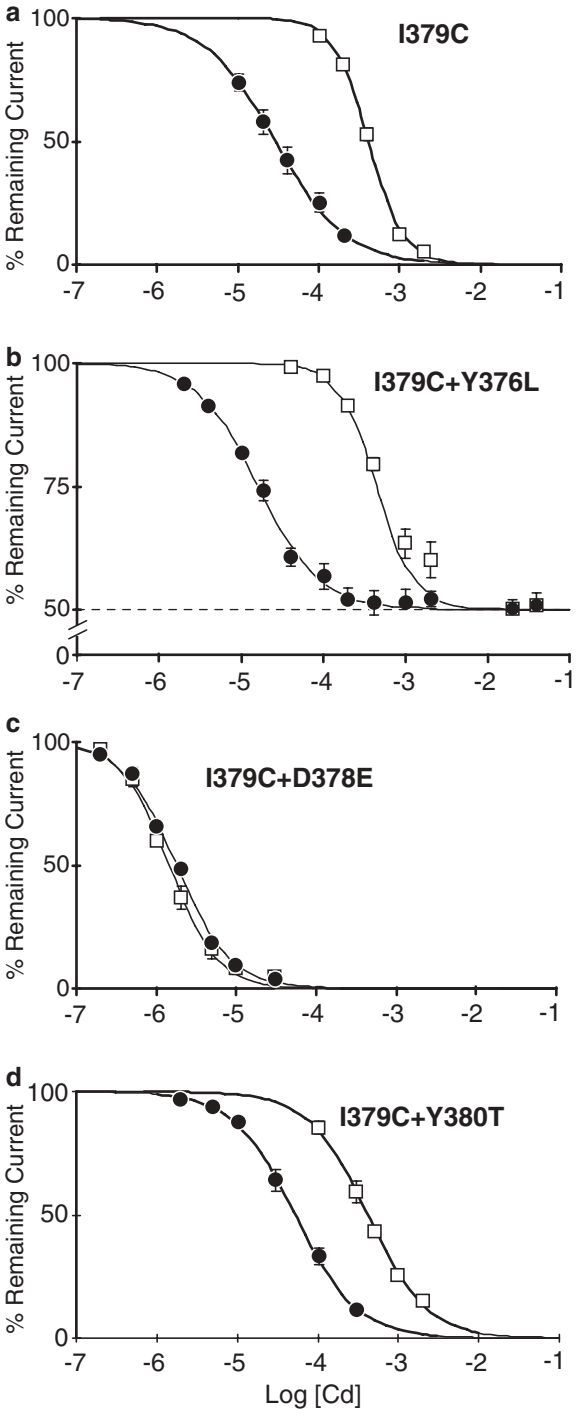

◀

Fig. 4 Aspartate D378 is critical for the K^+–Cd^{2+} antagonism. The effect of additional point mutations on the K^+–Cd^{2+} antagonism seen in I379C was evaluated by comparing the Cd^{2+} sensitivity in 100 mM external Na^+ and K^+. Currents were elicited by a 300 ms step depolarization to +40 mV from a holding potential of −80 mV. Cadmium concentration–inhibition curves were fitted with the Hill equation. **a** In the parent channel I379C, the Cd^{2+} concentration–inhibition curve is shifted rightward in 100 mM external K^+, compared to 100 mM Na^+, indicating K^+-selective antagonism of Cd^{2+} inhibition. **b** The same analysis as shown in (**a**), for I379C + Y376L. Interestingly, the efficacy of Cd^{2+} inhibition was 51% for this double mutant. External K^+ ions still selectively antagonize Cd^{2+} inhibition. **c** The same analysis as shown in (**a**) for I379C + D378E. The concentration–inhibition curves for 100 mM external Na^+ and K^+ overlap. Both are left-shifted compared with the 100 mM external NaCl curve in panel (**a**). **d** The same analysis as shown in (**a**) for I379C + Y380T. K^+ ions still effectively antagonize Cd^{2+} inhibition

the selectivity filter. Their electrostatic properties and dimension suggest that they could form the K^+-binding sites functionally described in this paper. Interestingly, similar cavities have recently been reported to surround the shaft of bacteriorhodopsin [60], where they allow dynamic changes of the shaft diameter and thereby support the catalytic cycle.

In conclusion, there appear to be two distinct candidate locations for the K^+- binding sites described here, the selectivity filter and the small cavities that surround it. Additional experiments were performed in order to find support for either possibility.

Altering the K^+/Rb^+ conductance ratio by mutating the selectivity filter

Mutation of residues in the pore-forming region of Kv2.1 to the amino acids found in the Kv4.1 K^+ channel (**TI**TMTT**V** to **VV**TMTT**L**) increases the single-channel K^+ conductance nearly three-fold to that of Kv4.1 [10, 40]. The last amino acid mutated in this region (V374L) corresponds to V76 in KcsA, the second residue of the selectivity filter which contributes its backbone carbonyl oxygen to K^+-binding site S2. This deep-pore mutation, which we have previously termed *drk1-L* [40], also significantly alters the selectivity profile for permeant ions. Whereas the K^+ conductance is increased by this mutation, the Rb^+ conductance is reduced, resulting in a five-fold increase of the K^+/Rb^+ conductance ratio (Fig. 7). If the K^+-binding sites that allosterically interact with Cd^{2+} ions in I379C are localized to the selectivity filter, then a change in the selectivity profile of the channel should result in a concomitant alteration of the profile for the antagonism of Cd^{2+} inhibition. The mutation that introduces the Cd^{2+}-binding site was therefore made in the drk1-L background. When we characterized this double mutant, drk1-L + I379C, in external solutions containing different monovalent cations, we found a severe rundown of the K^+ current in the absence of external K^+ ions. After switching to a 100 mM external NaCl solution, the outward current decreased to zero following an exponential time course with a time-constant of 24 s (data not shown). The rundown appeared to be irreversible, since the outward current did not recover by returning to a K^+-containing external solution. The minimal concentration of K^+ ions sufficient to prevent rundown was found to be 2 mM. External NaCl solutions were therefore supplemented with 2 mM KCl for all

Table 2 Cd^{2+} IC_{50} s (in μM) and Cd^{2+} Hill coefficients for Kv2.1 mutants in external Na^+ and K^+

Construct	IC_{50} Na	Hill Na	IC_{50} K	Hill K	IC_{50} K/IC_{50} Na
I379C	29.0	1.0	414	2.0	14.3
Y376L + I379C	16.1	1.2	445	1.9	27.7
D378E + I379C	1.8	1.3	1.4	1.5	0.8
Y380F + I379C	76.3	1.0	776	2.0	10.2
Y380T + I379C	52.3	1.1	415	1.2	7.9

the remaining experiments. Cd^{2+} inhibition in the drk1-L + I379C mutant developed much more slowly than in I379C (Fig. 8a, b), and recovery from the Cd^{2+} block was also extremely slow (data not shown). The equilibrium dissociation constant (K_D) for Cd^{2+} ions was therefore determined by analyzing the rate of Cd^{2+}

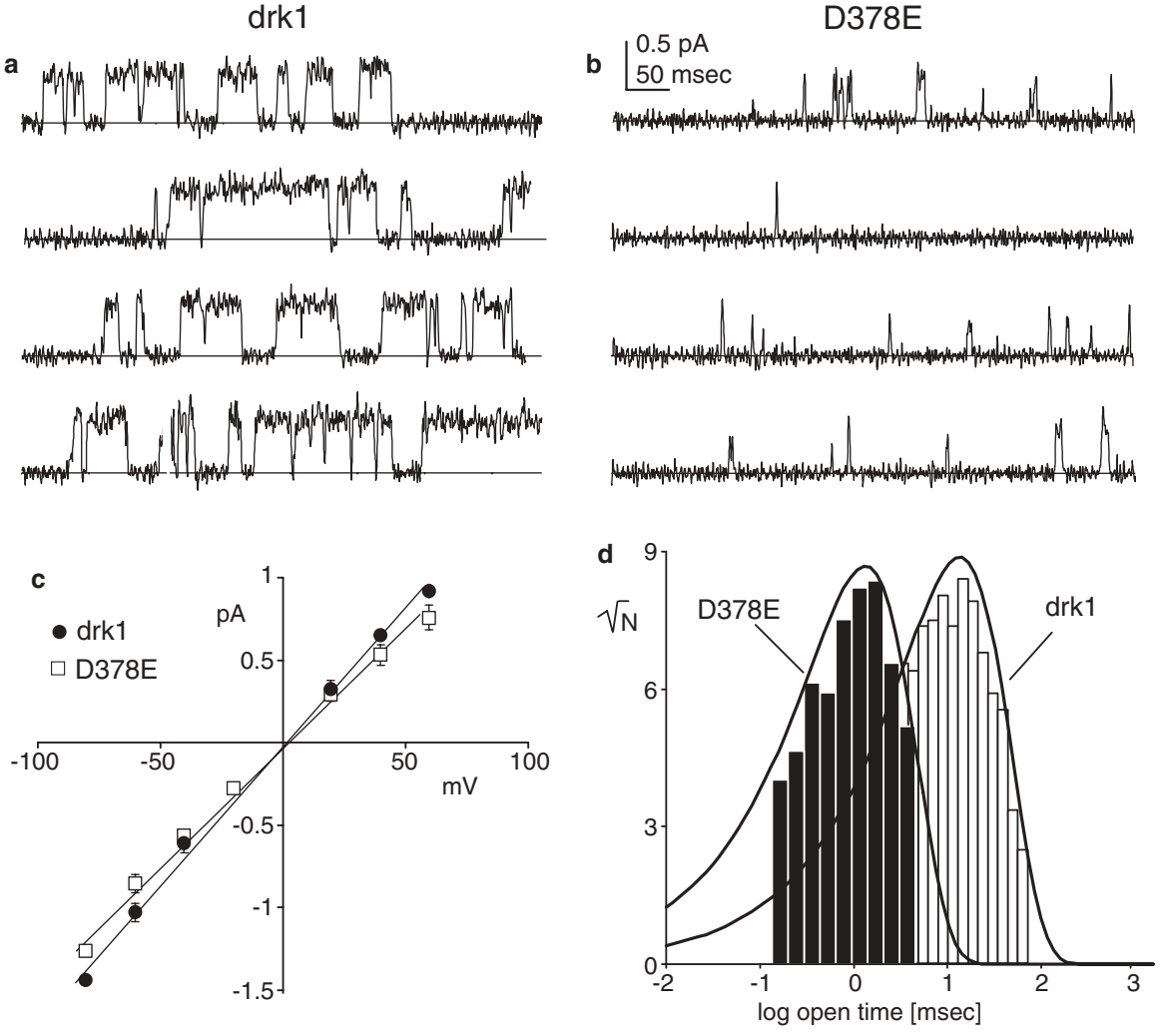

Fig. 5 D378E destabilizes the open state. **a** Representative single channel recordings of wild-type drk1 showing the typical behavior of the channel at 0 mV. Recording were made in cell-attached patches using 10 mM external KCl solution (see "Methods"). Channels that were recorded were activated by a 400-ms step depolarization from a holding potential of -80 mV. **b** Representative single channel recordings of the D378E mutant showing the markedly decreased mean open times of the channel at 0 mV. Experimental conditions were the same as in panel (**a**). **c** Single channel *I–V* relationship of Kv2.1 and D378E in isotonic 160 mM K^+. The *I–V* relationship was linear over a 160-mV range. *Data points* represent the mean ± SEM of 3–7 observations. *Solid lines* are simple linear regressions of the data with slopes of 14.3 ± 0.4 pS (D378E) and 15.5 ± 0.4 pS (Kv2.1). **d** Representative open time histograms of Kv2.1 and D378E. Histograms are shown as Sigworth–Sine transforms [77]. Data were taken from recordings at 0 mV with 10 mM external K^+. Kv2.1 data were scaled to match the number of D378E events for the purpose of comparison. Under these conditions, Kv2.1 was found to have a mean open time of 14.8 ± 0.3 ms ($n = 4$). The open time of D378E was reduced more than eightfold to 1.8 ± 0.3 ms ($n = 4$)

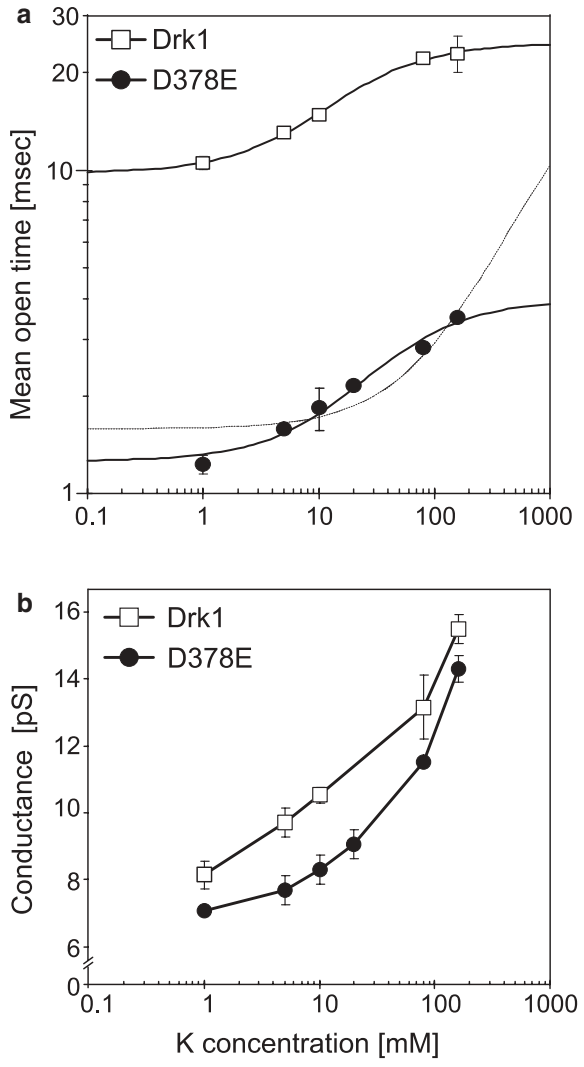

Fig. 6 $[K^+]_o$-dependence of gating and permeation. **a** Log–log plot of mean open times of Kv2.1 and D378E as a function of external K^+ concentration, $[K^+]_o$. Data were pooled over voltages from 0 to +60 mV as no voltage -dependence of mean open time was observed in this voltage range. Data points represent the mean ± SEM of 3–11 observations. External solutions (pipette solutions) were made by substitution of KCl for NMDG-Cl with osmolarity held constant. Open times of Kv2.1 were 6.5- to 8.5-fold longer than D378E at each concentration. The data for Kv2.1 and D378E were fit with the Hill equation (see Fig. 1), with the Hill coefficient fixed at 1. Optimal models are indicated by *solid continuous lines*. The K^+ EC_{50} was 18.9 mM for Kv2.1 and 43 mM for D378E. The lower/upper asymptotes were 9.8/14.9 ms for Kv2.1 and 1.3/2.7 ms for D378E. The data for D378E are not consistent with a model in which only the EC_{50} was altered, with no effect on the upper asymptote (*dotted line*). It appears therefore that the D378E mutation has caused a small right-shift in the EC_{50} and severely altered the range over which K^+ ions binding at the external site modulate single channel gating. However, D378E did not remove the K^+ modulation of the open-state stability. **b** Semi-logarithmic plot of single channel conductance of Kv2.1 and D378E vs $[K^+]_o$. Data points represent the mean ± SEM of slope or chord conductances ($n = 3$–7 for each point). The $[K^+]_o$-dependent increase of conductance observed in Kv2.1 was also seen in D378E. For all K concentrations tested, the single channel conductance was smaller for D378E than for the wild-type channel

inhibition at several Cd^{2+} ion concentrations, which also yielded microscopic on- and off-rate constants (Fig. 8c, d). Both the Cd^{2+} on- and off-rates were significantly smaller in drk1-L + I379C than in I379C, but the K_D was actually two-fold lower. Next, the ability of K^+ and Rb^+ to antagonize Cd^{2+} inhibition was evaluated for drk1-L + 379C (Fig. 9). Whereas K^+ and Rb^+ ions are both quite effective in relieving Cd^{2+} inhibition in I379C (Fig. 1), in the drk1-L background the effectiveness of Rb^+ ions to antagonize Cd^{2+} inhibition is significantly reduced (Fig. 9). This reduction mirrors the reduction in Rb^+ conductance produced by the drk1-L mutation (Fig. 7).

Discussion

Experiments on wild-type and mutant Kv2.1 (drk1) K^+ channels were described that revealed two effects of external K^+ ions: modulation of single-channel gating by altering the open-state stability, and antagonism of Cd^{2+} inhibition in a Kv2.1 cysteine substitution mutant, I379C. In order to understand the allosteric interaction between external K^+ ions and Cd^{2+} ions (Fig. 3), the mechanism of Cd^{2+} inhibition will be considered first.

The nature of Cd^{2+} inhibition in Kv2.1-I379C

The I379C mutation introduces four novel thiol groups in the homo-tetrameric Kv2.1 K^+ channel. Thiols have a high affinity for soft-metal divalent cations, including Cd^{2+} and Zn^{2+}, and their coordination chemistry allows for up to four thiol groups per cation [51]. However, the shortest distance between neighboring cysteines at position 379 is predicted to be 16 Å, prohibiting the coordination of bound Cd^{2+} ions by more than one thiol. The relatively low affinity for Cd^{2+} of I379C is also consistent with the soft-metal divalent being bound by a single-thiol ligand: proteins that contain a soft-metal-binding site employing four cysteines (i.e., zinc-finger domains) display picomolar affinities, while a Kv2.1 dimer (I379C-Y380C) that introduces a inter-subunit metal bridge containing two cysteines binds the cadmium ions with nanomolar affinity [51]. It is therefore likely that there are four equivalent Cd^{2+}-binding sites per channel. How does a Cd^{2+} ion coordinated by the thiol at position 379 inhibit outward K^+ currents? An open-channel blocking mechanism is unlikely, due to their large distance to the filter and the side-chain orientation of position 379. Instead, Cd^{2+} ions most likely interfere with channel function allosterically, either by reducing the single-channel conductance, or by inhibiting channel gating. Additional experiments will be needed to distinguish between these two mechanisms. The allosteric nature of the Cd^{2+} inhibition is underscored by the data obtained for the double mutant I379C + Y376L (Fig. 3b). In this mutant, saturating

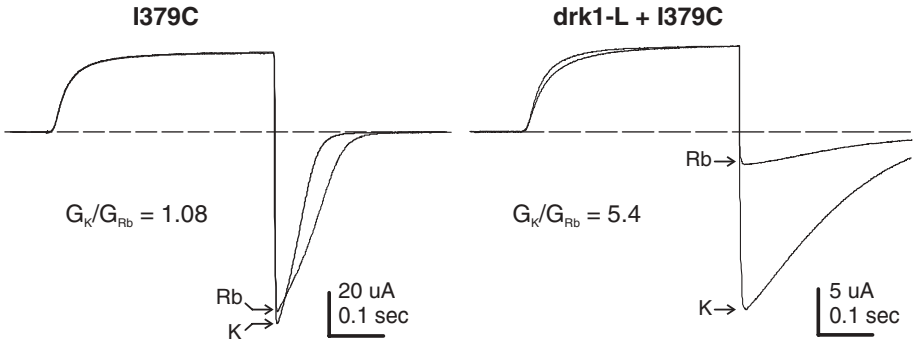

Fig. 7 Mutation drk1-L has a reduced Rb conductance. The potassium/rubidium -conductance ratio (G_K/G_{Rb}) was determined for Kv2.1-I379C (panel **a**) and the double mutant drk1-L + I379C (panel **b**). Outward K^+ currents and inward tail currents carried by either K^+ or Rb^+ ions were elicited by 400- ms step depolarizations to +40 mV, followed by a repolarization to −120 mV. The external solution contained 100 mM KCl or 100 mM RbCl, to which was added 2 mM $MgCl_2$ and 10 mM HEPES (pH 7.4). The current traces in external K^+ and Rb^+ were overlaid following normalization of the outward K^+ current. *Arrows* indicate the size of the inward K^+ and Rb^+ tail currents which was used to calculate the K^+/Rb^+ conductance ratio

Cd^{2+} concentrations are only able to inhibit outward K^+ currents by 50%, which is incompatible with a mechanism involving open-channel block. Despite this reduction in the effectiveness of the allosteric Cd^{2+} effect, external K^+ ions still selectively and efficiently antagonize the inhibition in the I379C + Y376L double mutant. It is concluded that I379C introduces four Cd^{2+}-binding sites in the external vestibule of Kv2.1 that inhibit K^+ channel function through an allosteric mechanism.

The nature of external K^+ antagonism of Cd^{2+} inhibition

External K^+ ions mediate their antagonistic effect on Cd^{2+} inhibition through a site that selectively binds permeant ions, although the selectivity profile is distinct from the channel itself (Fig. 1). The binding of K^+ to this site was weakly voltage-dependent (Fig. 2b), indicating that bound K^+ ions experience 7% of the membrane electric field, or that they are coupled to the movement of K^+ ions through the filter. The two most external K^+- binding sites associated with the filter (S1 and S0) are predicted to possess these properties. The efficacy of K^+ ions to antagonize Cd^{2+} increased with decreasing ionic strength (Fig. 2a), suggesting that K^+ and Cd^{2+} ions do not compete directly for the same binding site. The existence of distinct sites for Cd^{2+} and K^+ ions is consistent with the finding that their interaction could be well described by a model for allosteric competitive antagonism (Fig. 3). Finally, thiols are excellent ligands for soft-metal divalent cations like Cd^{2+}, while they bind K^+ ions poorly. Taken together, this leads us to conclude that K^+ ions bind to a site that is distinct from the one introduced by the cysteine substitution I379C. The Hill coefficient describing K^+ binding was greater than unity (Figs. 1, 3, Table 1), indicating that external K^+ ions mediated their effect by interacting with a composite of at least two interacting binding sites.

Functional roles for D378

Aspartate 378 was found to be a critical determinant for the effect of external K^+ ions on Cd^{2+} inhibition (Fig. 4). In addition to removing the Cd^{2+}–K^+ antagonism, the D378E mutation had a second consequence: it altered the single-channel gating behavior by destabilizing the open state and reducing the open probability (Fig. 5). Although the D378E mutation is immediately adjacent to the selectivity filter, there was no significant effect on K^+ permeation rate or ion selectivity. Because this aspartate (D80 in KcsA) is as highly conserved amongst K^+ channels as the amino acids that line the selectivity filter, this residue may be critical for the stability of the structure of the selectivity filter. If the selectivity filter is a dynamic structure that is actively involved in channel opening, as we have suggested previously [39, 40, 61, 62], then a destabilizing effect of D378E would help explain its gating phenotype.

The gating phenotype of D378E is not unique: point mutations at five of the six amino acids forming the selectivity filter (TVGYGD in Kv2.1) have been reported to severely alter single-channel gating. Mutation of the threonine in position 1 to serine (T1S) in *Shaker* [46] and mutation V2L in drk1 [40] greatly stabilize channel openings and reveal subconductance states. Backbone mutations of the glycine residues (G3 and G5) using non-natural amino acids severely altered the single-channel gating behavior of an inward rectifying K^+ channel [47]. Mutation of G3 in KcsA to D-alanine increases the dependence of the open probability on external Na^+ ions [63]. Finally, mutation of Y5 in a Kv2.1 tandem dimer construct reduced the single-channel conductance to such an extent that the channel openings could not be resolved and the effect on gating

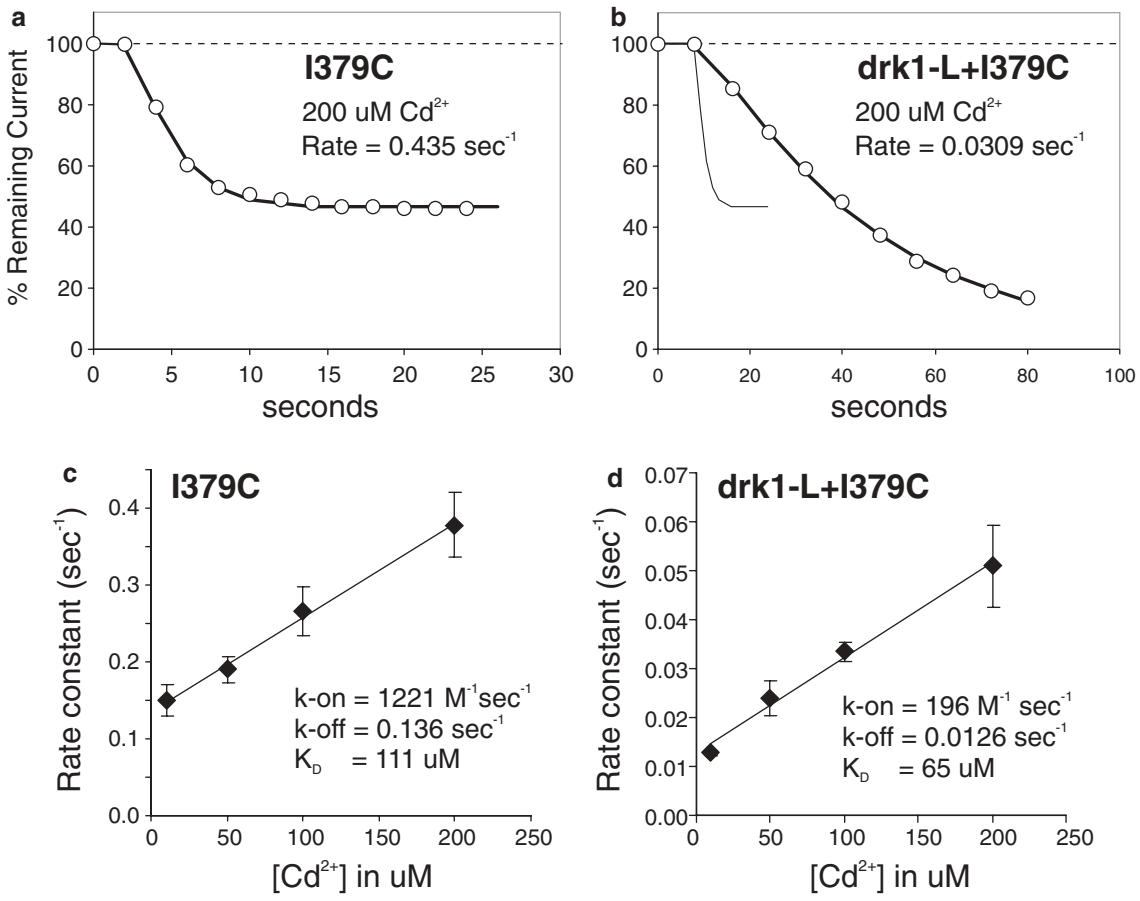

Fig. 8 Cd-inhibition in I379C and drk1-L + I379C. Cd^{2+} inhibition was characterized in the double mutant drk1-L + I379C. The external solution contained 100 mM NaCl, 2 mM KCl, 2 mM $MgCl_2$ and 10 mM HEPES (pH 7.4). A small amount of K^+ ions was required to prevent irreversible rundown (see text). **a**, **b** Inhibition of outward K^+ current by 200 μM Cd^{2+} developed significantly more slowly in the drk1-L background (panel **b**) than in the wild -type background (panel **a**). Note the different time axes in (**a**) and (**b**). The time-course of Cd^{2+} inhibition in I379C is shown as a *thin line* in panel (**b**) for comparison. **c**, **d** The rate constants of Cd^{2+} inhibition were measured for four Cd^{2+} concentrations in five oocytes. The mean values were graphed against Cd^{2+} concentration and fitted with a straight line. The slope and *Y*-intercept yield estimates for the microscopic on-rate and off-rate constants, respectively. The equilibrium dissociation constant K_D is then calculated as k_{off}/k_{on}. Both the on- and off-rates are significantly slower in the drk1-L background, but the K_D is smaller

could not be evaluated [64]. Together with the gating phenotype of D378E reported here, these results imply that the TVGYGD selectivity filter region plays a critical role in defining the parameters that govern single-channel open/close behavior.

The aspartate residue that is identified here as a critical component of the effects of external K^+ ions (D378 in Kv2.1, D447 in *Shaker* and D80 in KcsA), is the terminal residue of the K^+ channel GYGD "signature sequence". It is absolutely conserved in voltage-gated K^+ channels and present in many, but not all, K^+ channels not gated by voltage [64]. Site-directed mutagenesis of this position has shown that only the charge-conserving glutamate substitution yields functional channels [64]. Even the structurally conservative asparagine mutation, which maintains side-chain volume but neutralizes the negative charge, yields a non-conducting channel. This non-conducting variant of the *Shaker* K^+ channel (D447 N) does, however, display gating currents [65] and Ba^{2+} modulation of gating charge movement is mediated by this aspartate residue [65]. External K^+ ions can also affect the rate of gating charge return in Kv1.5 [66], potentially through an interaction with D447.

External K^+ ions alter single-channel gating

The dual phenotype of D378E, loss of K^+ antagonism of Cd^{2+} inhibition and altered single-channel gating, suggested that the two phenomena could be linked. Indeed, it was found that external K^+ ions modulate single-channel gating behavior, with increasing K^+ concentrations producing more stable openings. The K^+-dependence is fairly shallow: a 100-fold increase in the external K^+ concentration (from 1 to 100 mM) re-

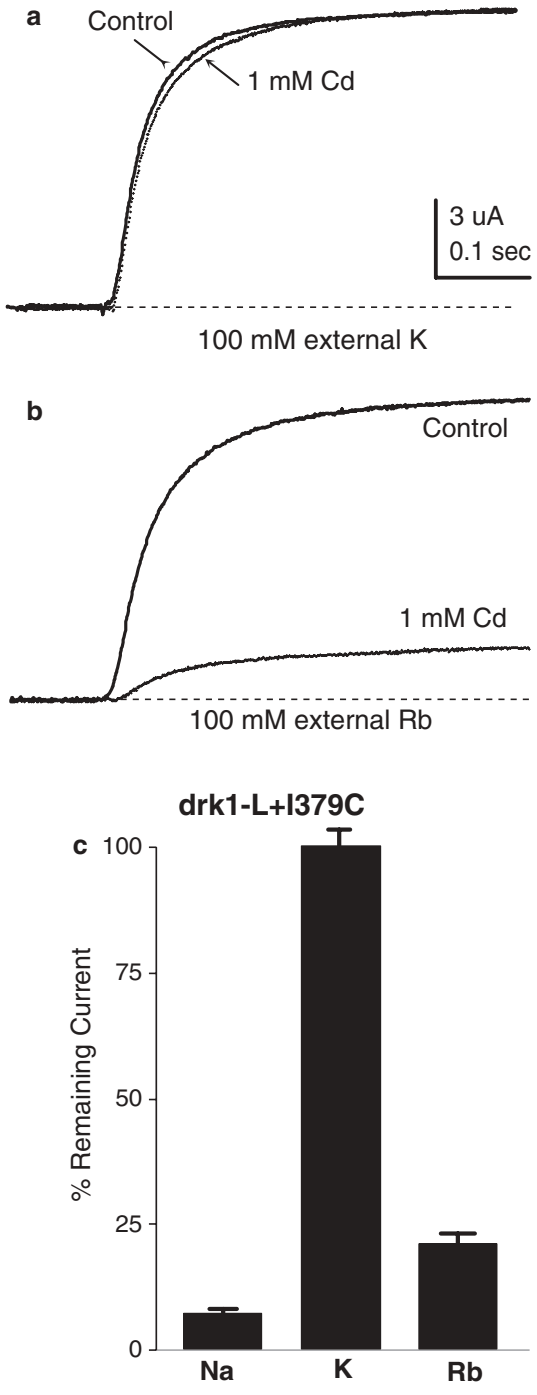

Fig. 9 Reduced effectiveness of Rb to antagonize Cd-inhibition in drk1-L + I379C. **a** Outward K currents elicited by a step depolarization to +40 mV from a holding potential of −80 mV for the double mutant drk1-L + I379C. The external solution was 100 mM KCl, 2 mM $MgCl_2$ and 10 mM HEPES (pH 7.4). Two current traces are shown, before and after the addition of 1 mM $CdCl_2$. At a concentration of 100 mM, external K^+ ions completely prevent inhibition by Cd^{2+} ions. **b** The same experiment as in (**a**), except that KCl in the external solution was replaced with 100 mM RbCl; 1 millimolar Cd^{2+} ions now inhibit 75% of the outward K^+ current. **c** *Bar histogram* illustrating the percentage current remaining after block by 1 mM Cd^{2+} in external solutions containing 100 mM NaCl + 2 mM KCl (Na), 100 mM KCl (K) or 100 mM RbCl (Rb)

sulted in only a 2.2-fold increase in the mean open time (Fig. 6). The D378E mutation did not remove the external K^+ concentration-dependence of the mean open time. Instead, it increased the EC_{50} two-fold and greatly shifted the range over which K^+ ions can modulate the open time (Fig. 6). The K^+-dependence remains shallow, with the mean open time increasing 2.6-fold when going from 1 to 100 mM external K^+. Whereas the aspartate at position 378 is critical for the K^+–Cd^{2+} antagonism in I379C, both an aspartate and a glutamate at this position support the effect of external K^+ ions on gating. This prompts the question whether the dual effects of external K^+ ions, antagonism of Cd^{2+} inhibition and modulation of single-channel gating, are mediated by a single K^+-binding site or by two distinct binding sites?

Where is the composite K^+-binding site?

We have discussed two possible locations for an external K^+-binding site: the selectivity filter or the small cavities that surround it. Crystallographic structures of several other proteins containing K^+-binding sites (1AQF.pdb, 1AX4.pdb and 1JDR.pdb) display a coordination sphere containing a single aspartate or glutamate side chain, complemented by a set of backbone carbonyl oxygens. It is therefore conceivable that the side chain of D378 could directly coordinate a K^+ ion if it were to reside in one of the small cavities surrounding the selectivity filter. Although molecular dynamics simulations have revealed the presence of water molecules in these cavities [67], K^+ ions were not reported to enter them. In addition, the cavities are too small to accommodate a fully hydrated K^+ ion. Entry in these cavities would therefore require a partial dehydration and it is not clear by which mechanism this may occur.

The results presented here using the drk1-L mutant also point toward the selectivity filter as the more likely location for the K^+-binding sites that mediate the antagonism between external K^+ ions and Cd^{2+} ions. The properties of the K^+-binding sites in the selectivity filter are altered in the drk1-L mutant, since the K^+/Rb^+ conductance ratio is increased from 1 to 5.4 (Fig. 7). The reduction of the Rb^+ conductance in drk1-L was mirrored by a similar reduction in the effectiveness with which Rb^+ ions antagonize Cd^{2+} inhibition in drk1-L + I379C (Fig. 9). This finding strongly supports the hypothesis that the K^+-binding sites that mediate the K^+–Cd^{2+} antagonism are localized to the selectivity filter.

Other effects of external K^+ ions on K^+-channel function

External K^+ ions have been described to modulate a number of K^+-channel functional properties. D378 in Kv2.1 may be involved in some of these phenomena. External K^+ ions can induce conformational

rearrangements of the external vestibule in Kv2.1 that affect TEA binding [33] and K^+ current magnitude [38], and these effects have been suggested to be mediated by a low-affinity, external K^+-binding site associated with the selectivity filter [68]. C-type inactivation [25, 28, 69] has been shown to be antagonized by external K^+ ions [70]. C-type inactivation can also be altered by mutagenesis of the following residues in or near the pore (KcsA numbering): W67, Y78 and Y82 [65, 71–74]. Together, these positions make up the local environment of aspartate D80 in KcsA. These published findings, together with the data presented here, prompt a number of questions. First, is there a relationship between D80, W67, Y78 and Y82 that can explain their role in C-type inactivation? And second, what is the mechanism by which external K^+ ions modulate Cd^{2+} inhibition in Kv2.1-I379C (Fig. 1), mean open time in wildtype Kv2.1 (Fig. 6), TEA binding and C-type inactivation? A potential answer was provided by an analysis of the KcsA structure.

An inter-subunit H-bond network involving D80, W67 and Y78

In tandem-pore domain K^+ channels, the amino acid at the D80 position fine-tunes the K^+ selectivity through a functional interaction with the central tyrosine (Y78) in the selectivity filter of the neighboring subunit [64]. D80 immediately follows the TVGYG selectivity filter sequence and it does not directly contact the K^+ ions. In KcsA, aspartate D80 is involved in a carboxyl–carboxylate bridge with glutamate E71 in the pore helix [75]. However, voltage-gated K^+ channels contain a neutral amino acid at position 71, which prevents D80 from forming an equivalent linkage. We have therefore analyzed the environment of D80 in the KcsA structure following mutation of glutamate 71 to alanine. In addition, we evaluated the effect of mutations L81C and D80E, the equivalents of I379C and D378E in Kv2.1 which were functionally characterized in this paper. In KcsA-E71A, D80 is predicted to form a hydrogen bond with tryptophan W67 in the pore helix of the same subunit (Fig. 10a). The neighbor of W67 is tryptophan W68, which forms an inter-subunit H-bond with Y78′ [16], the tyrosine in the center of the selectivity filter. A rigid-body rotation of the pore helix will simultaneously disrupt the D80–W67 and W68–Y78′ H-bonds. Consequently, D80 and Y78′ help stabilize the pore helix in the conformation shown. It is therefore proposed that the inter-subunit H-bond network formed by D80–W67∼W69–Y78′ may underlie the functional interaction between the D80 position and Y78 in the neighboring subunit [61].

In Kv2.1, the cysteine-substitution I379C introduces a soft-metal binding site (Fig. 1). The equivalent mutation in KcsA, L81C, allows the side chain of D80 to form an alternative H-bond with the introduced thiol (Fig. 10b). Analysis of the KcsA-L81C structure suggests that a soft-metal divalent cation (e.g., Cd^{2+}) coordinated by the thiol at position 81 would likely recruit a carboxyl oxygen of the D80 side chain, preventing it from forming an H-bond with W67. Binding of Cd^{2+} ions is therefore expected to negatively affect the stability of the inter-subunit H-bond network, thereby providing an allosteric mechanism for inhibiting K^+ channel function by disrupting the D80–Y78′ interaction (Fig. 10a). A mutation of the D80 equivalent in Kv2.1, D378E, had two phenotypes: it reduced the mean open time and also removed the effect of external K^+ ions on Cd^{2+} inhibition in I379C. Analysis of KcsA-D80E revealed that a glutamate residue at position 80 is not capable of forming a H-bond with tryptophan W67, and therefore the inter-subunit H-bond network shown in Fig. 10a that allows D80 to interact with Y78 does not exist. In the D80E + L81C double mutant, the most stable conformation involves an H-bond between E80 and C31 (Fig. 10c). These structural observations led to the following allosteric model.

A model for the allosteric interaction between external K^+ and Cd^{2+} ions

The model is based on the following considerations. The aspartate immediately following the selectivity filter TVGYG sequence, D378 in Kv2.1 and D80 in KcsA, is able to functionally interact with tyrosine Y78, through an inter-subunit H-bond network (Fig. 10a). It is proposed that this network allows D378 to mediate the allosteric interaction between Cd^{2+} ions bound to the thiol introduced by I379C and external K^+ ions binding to sites in the selectivity filter. Mechanistic details of the model are explained in the legend to Fig. 11. The allosteric interaction is bi-directional: bound Cd^{2+} ions negatively affect the function of the selectivity filter, inhibiting outward K^+ currents and the external K^+ ions antagonize the Cd^{2+} effect by altering the relative occupancy of the K^+-binding sites in the filter. The allosteric interaction is lost in the D378E mutation because a glutamate at position 80 is unable to from a H-bond with W67 (Fig. 10c), which prevents the H-bond network from functioning. D378E does not remove a K^+-binding site, but instead eliminates the coupling between the Cd^{2+}-binding site and the K^+ sites in the filter. The effect of external K^+ ions on the mean open time and the significant effect on single-channel gating of the D378E mutations can be explained in terms of this model if the selectivity filter is critically involved in opening the channel, as we have previously proposed [39, 40, 62].

Conclusions

It is proposed that the aspartate residue immediately following the TVGYG selectivity filter region plays a

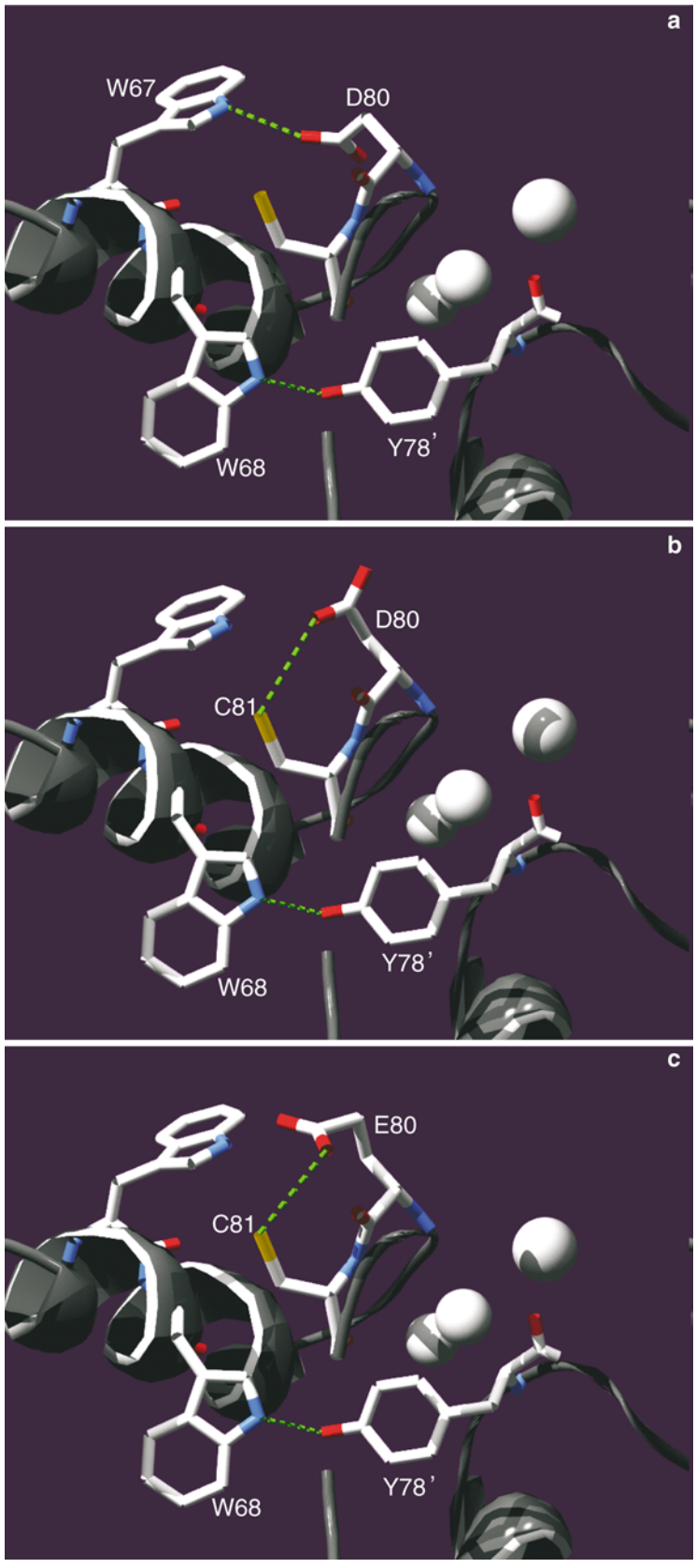

Fig. 10 An inter-subunit H-bond network involving D80. The immediate environment of D80 was analyzed in the KcsA-E71A mutant K^+ channel. The figures show *CPK-colored stick representations* of relevant side chains and a *ribbon representation* of the peptide backbone. Three K^+ ions in the selectivity filter are shown as *spheres*. **a** In KcsA-E71A, the most stable rotamer for D80 displays a H-bond between a carboxyl oxygen of the D80 side chain with the cyclic amine of tryptophan W67 localized in the pore helix of the same subunit. The length of the H-bond is 3.0 Å and is indicated by a *green dotted line*. The neighbor of W67 is tryptophan W68, which forms an inter-subunit H-bond with Y78′ [16], the tyrosine in the center of the selectivity filter. **b** The equivalent mutation of Kv2.1-I379C in KcsA is L81C; it allows the side chain of D80 to form an alternative H-bond with the introduced thiol, indicated by a *green dotted line*. The length of this H-bond is 3.27 Å and it is energetically less favorable than the D80–W67 H-bond shown in panel (**a**). **c** Analysis of the KcsA double mutant D80E + L81C, equivalent to Kv2.1-D378E + I379C, revealed that a glutamate at position 80 is not capable of forming an H-bond with W67. The most favorable conformation now involves an H-bond between the side chains of E80 and C81

pivotal role in a number of channel functions, including fine-tuning the ion selectivity [64], setting the open state stability and mediating the effects of external K^+ ions on Cd^{2+} inhibition by a functional interaction with the central tyrosine of the selectivity filter. External K^+ ions affect channel function by altering the

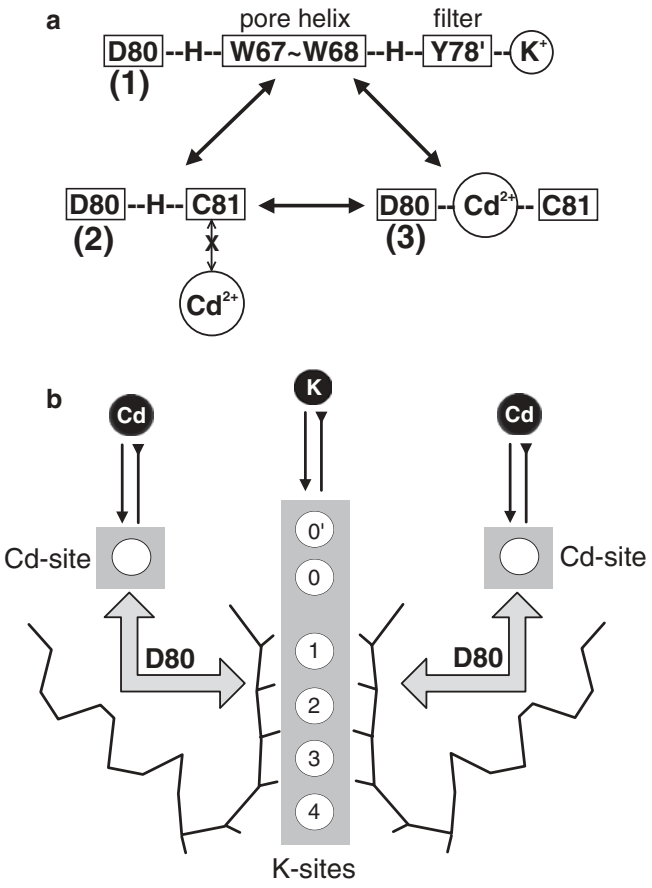

Fig. 11 Model for the allosteric interaction between external K^+ and Cd^{2+} ions in I379C. **a** Analysis of the structural environment of D80 (Fig. 10) revealed that it can be involved in several mutually exclusive interactions, which are illustrated here. Interaction **(1)** involves an H-bond between D80 and W67 in the pore helix of the same subunit. The amino acid following W67 is W68, which forms a H-bond with Y78 in the selectivity filter of the neighboring subunit [16]. The backbone carbonyl oxygen of Y78 contributes to sites S1 and S2 in the filter and directly contacts a K^+ ion. The four Y78–W68 H-bonds in the filter act as springs, holding the pore open at a diameter that is optimal for coordinating a dehydrated K^+ ion, while preventing the oxygens from closing in enough to support the smaller Na^+ ion [16]. This spring action implies that the W68–Y78 H-bond and the coordination of a K ion by Y78 are energetically coupled. The D80–W67∼W68–Y78′ H-bond network may therefore allow D80 to "sense" the occupancy profile of the filter. Interaction **(2)** involves a H-bond between D80 (D378) and C81 (the cysteine substituted for I379). Because the H-bond forms between a carbonyl oxygen of the D378 side chain and the thiol moiety of C379, it prevents the thiol from coordinating a Cd^{2+} ion. Interaction **(3)** involves the recruitment of D378 side-chain oxygens by a bound Cd^{2+} ion. Interactions (2) and (3) allow D378 to modulate Cd^{2+} binding. The D378 side chain can only be involved in one of these three interactions. The amount of time spent in each configuration depends on their relative stability. **b** Schematic representation of a model proposed to explain the data presented in this paper. External K ions mediate their effect by altering the occupancy profile of the K^+ binding sites in the selectivity filter (S0–S4), represented here schematically by a backbone trace of two of the four subunits. Mutation I379C introduces four equivalent Cd^{2+}-binding sites in the external vestibule. A Cd^{2+} ion bound to one of these sites is coordinated by a single thiol group of cysteine 379 and Cd^{2+} binding may be further stabilized by recruitment of the negatively charged side chain of D378 (panel **a**). Aspartate 378 acts like a molecular switch with three configurations, which either allow, prevent or promote Cd^{2+} binding (interactions (1), (2) and (3) in panel **a**, respectively). The relative free energy of each interaction determines which one will predominate. The inter-subunit H-bond network (Fig. 10a) allows external K ions to affect the stability of the W67–D80 H-bond (interaction (1) in panel **a**) and thereby modulate Cd^{2+} binding. In this model, the selectivity filter is allosterically coupled to the Cd^{2+}-binding site (illustrated by the *gray arrow on the right side of the cartoon*). Because an allosteric coupling is predicted to be bi-directional, the same H-bond network may also mediate the allosteric inhibition of K channel function exerted by bound Cd^{2+} ions. However, our data do not provide further support for this idea. The model does explain the phenotype of the D378E mutation. A glutamate at position 80 in KcsA is not able to form an H-bond with W67 (Fig. 10), implying that interaction (1) in panel (**a**) is not allowed in the D378E mutant K channel. Without an allosteric coupling between the filter and the binding site, external K ions can no longer antagonize Cd^{2+} inhibition. External K ions are not prevented from binding to the filter in the D378E mutant, and therefore can still exert their effect on open state stability

occupancy of the sites in the filter and inducing conformational changes in the external vestibule through an inter-subunit H-bond network. These data add further support for the idea that the external vestibule and selectivity filter are dynamic structures [18, 33, 38, 57, 75] critically involved in many aspects of channel function.

Acknowledgements The authors wish to thank Leonardo Guidoni and Jane Richardson for helpful discussions. This work was supported by NIH grant NS031557 to AMJVD.

References

1. Hodgkin AL, Huxley AF (1952) A quantitative description of membrane current and its application to conduction and excitation in nerve. J Physiol (Lond) 117:500–544
2. Papazian DM, Timpe LC, Jan YN, Jan LY (1991) Alteration of voltage-dependence of Shaker potassium channel by mutations in the S4 sequence. Nature 349:305–310
3. Logothetis DE, Movahedi S, Satler C, Lindpaintner K, Nadal-Ginard B (1992) Incremental reductions of positive charge within the S4 region of a voltage-gated K channel result in corresponding decreases in gating charge. Neuron 8:531–540
4. Larsson HP, Baker OS, Dhillon DS, Isacoff EY (1996) Transmembrane movement of the Shaker K^+ channel S4. Neuron 16:387–397
5. Yang N, George AL Jr, Horn R (1996) Molecular basis of charge movement in voltage-gated sodium channels. Neuron 16:113–122
6. Bezanilla F (2000) The voltage sensor in voltage-dependent ion channels. Physiol Rev 80:555–592 (erratum appears in Physiol Rev 2000 July;80(3):following. Review 120 refs)
7. Jiang Y, Lee A, Chen J, Ruta V, Cadene M, Chait BT, Mackinnon R (2003) X-ray structure of a voltage-dependent K channel. Nature 423:33–41
8. Mackinnon R (1991) New insights into the structure and function of potassium channels. Curr Opin Neurobiol 1:14–19 (Review 37 refs)
9. Mackinnon R, Yellen G (1990) Mutations affecting TEA blockade and ion permeation in voltage-activated K^+ channels. Science 250:276–279
10. Hartmann HA, Kirsch GE, Drewe JA, Taglialatela M, Joho RH, Brown AM (1991) Exchange of conduction pathways between two related potassium channels. Science 251:942–944
11. Yellen G, Jurman ME, Abramson T, Mackinnon R (1991) Mutations affecting internal TEA blockade identify the probable pore-forming region of a K channel. Science 251:939–942
12. Yool AJ, Schwarz TL (1991) Alteration of ionic selectivity of a K channel by mutation of the H5 region. Nature 349:700–704
13. Liu Y, Holmgren M, Jurman ME, Yellen G (1997) Gated access to the pore of a voltage-dependent K^+ channel. Neuron 19:175–184
14. Holmgren M, Yellen G (1998) The activation gate of a voltage-gated K channel can be trapped in the open state by an intersubunit metal bridge. Neuron 21:617–621
15. del Camino D, Holmgren M, Liu Y, Yellen G (2000) Blocker protection in the pore of a voltage-gated K^+ channel and its structural implications. Nature 403:321–325
16. Doyle DA, Cabral JM, Pfuetzner RA, Kuo A, Gulbis JM, Cohen SL, Chait BT, Mackinnon R (1998) The structure of the potassium channel: molecular basis of K conduction and selectivity. Science 280:69–76
17. Yellen G (1998) Premonitions of ion channel gating. Nat Struct Biol 5:421
18. Perozo E, Cortes DM, Cuello LG (1999) Structural rearrangements underlying K^+-channel activation gating. Science 285:73–78
19. Perozo E, Cortes DM, Cuello LG (1998) Three-dimensional architecture and gating mechanism of a K^+ channel studied by EPR spectroscopy. Nat Struct Biol 5:459–469
20. Jiang Y, Lee A, Chen J, Cadene M, Chait BT, Mackinnon R (2002) Crystal structure and mechanism of a calcium-gated potassium channel. Nature 417:515–522
21. Swenson RP Jr, Armstrong CM (1981) K^+ channels close more slowly in the presence of external K^+ and Rb^+. Nature 291:427–429
22. Shapiro MS, DeCoursey TE (1991) Permeant ion effects on the gating kinetics of the type L potassium channel in mouse lymphocytes. J Gen Physiol 97:1251–1278
23. Pardo LA, Heinemann SH, Terlau H, Ludewig U, Lorra C, Pongs O, Stuhmer W (1992) Extracellular K^+ specifically modulates a rat brain K^+ channel. Proc Natl Acad Sci USA 89:2466–2470
24. Demo SD, Yellen G (1992) Ion effects on gating of the $Ca(2^+)$-activated K^+ channel correlate with occupancy of the pore. Biophys J 61:639–648
25. Lopez-Barneo J, Hoshi T, Heinemann SH, Aldrich RW (1993) Effects of external cations and mutations in the pore region on C-type inactivation of Shaker potassium channels. Receptors Channels 1:61–71
26. Gomez-Lagunas F, Armstrong CM (1994) The relation between ion permeation and recovery from inactivation of ShakerB K^+ channels. Biophys J 67:1806–1815
27. Pennefather PS, DeCoursey TE (1994) A scheme to account for the effects of Rb^+ and K^+ on inward rectifier K channels of bovine artery endothelial cells. J Gen Physiol 103:549–581
28. Baukrowitz T, Yellen G (1995) Modulation of K^+ current by frequency and external $[K^+]$: a tale of two inactivation mechanisms. Neuron 15:951–960
29. Jarolimek W, Soman KV, Brown AM, Alam M (1995) The selectivity of different external binding sites for quaternary ammonium ions in cloned potassium channels. Pflugers Arch 430:672–681
30. Clay JR (1996) Effects of permeant cations on K^+ channel gating in nerve axons revisited. J Membr Biol 153:195–201
31. Levy DI, Deutsch C (1996) Recovery from C-type inactivation is modulated by extracellular potassium. Biophys J 70:798–805
32. Hurst RS, Roux MJ, Toro L, Stefani E (1997) External barium influences the gating charge movement of Shaker potassium channels. Biophys J 72:77–84
33. Immke D, Wood M, Kiss L, Korn SJ (1999) Potassium-dependent changes in the conformation of the Kv2.1 potassium channel pore. J Gen Physiol 113:819–836
34. Ikeda SR, Korn SJ (1995) Influence of permeating ions on potassium channel block by external tetraethylammonium. J Physiol 486:267–272
35. Immke D, Korn SJ (2000) Ion–ion interactions at the selectivity filter. Evidence from $K(^+)$-dependent modulation of tetraethylammonium efficacy in Kv2.1 potassium channels. J Gen Physiol 115:509–518
36. Kiss L, Korn SJ (1998) Modulation of C-type inactivation by K^+ at the potassium channel selectivity filter. Biophys J 74:1840–1849
37. Kiss L, LoTurco J, Korn SJ (1999) Contribution of the selectivity filter to inactivation in potassium channels. Biophys J 76:253–263
38. Andalib P, Wood MJ, Korn SJ (2002) Control of outer vestibule dynamics and current magnitude in the Kv2.1 potassium channel. J Gen Physiol 120:739–755
39. VanDongen AMJ (1992) Structure and function of ion channels: a hole in four? Commun Theor Biol 2:429–451
40. Chapman ML, VanDongen HMA, VanDongen AMJ (1997) Activation-dependent subconductance levels in K channels suggest a subunit basis for ion permeation and gating. Biophys J 72:708–719
41. Taylor WR, Baylor DA (1995) Conductance and kinetics of single cGMP-activated channels in salamander rod outer segments. J Physiol 483:567–582
42. Rosenmund C, Stern-Bach Y, Stevens CF (1998) The tetrameric structure of a glutamate receptor channel. Science 280:1596–1599
43. Zheng J, Sigworth FJ (1998) Intermediate conductances during deactivation of heteromultimeric Shaker potassium channels. J Gen Physiol 112:457–474
44. Ferguson WB, McManus OB, Magleby KL (1993) Opening and closing transitions for BK channels often occur in two

steps via sojourns through a brief lifetime subconductance state. Biophys J 65:702–714
45. Schneggenburger R, Ascher P (1997) Coupling of permeation and gating in an NMDA-channel pore mutant. Neuron 18:167–177
46. Zheng J, Sigworth FJ (1997) Selectivity changes during activation of mutant Shaker potassium channel. J Gen Physiol 110:101–117
47. Lu T, Mainland J, Jan LY, Schultz PG, Yang J (2001) Probing ion permeation and gating in a K channel with backbone mutations in the selectivity filter. Nat Neurosci 4:239–246
48. Sarkar G, Sommer SS (1990) The "megaprimer" method of site-directed mutagenesis. Biotechniques 8:404–407
49. VanDongen AMJ, Frech GC, Drewe JA, Joho RH, Brown AM (1990) Alteration and restoration of K^+ channel function by deletions at the N- and C-termini. Neuron 5:433–443
50. VanDongen AMJ (1996) A new algorithm for idealizing single ion channel data containing multiple unknown conductance levels. Biophys J 70:1303–1315
51. Krovetz HS, VanDongen HMA, VanDongen AMJ (1997) Atomic distance estimates from novel disulfide bonds and high-affinity metal binding sites support a radial model for the K channel pore. Biophys J 72:117–126
52. Spassova M, Lu Z (1999) Tuning the voltage dependence of tetraethylammonium block with permeant ions in an inward-rectifier K channel. J Gen Physiol 114:415–426
53. Thompson J, Begenisich T (2003) External TEA block of Shaker K^+ channels is coupled to the movement of K^+ ions within the selectivity filter. J Gen Physiol 122:239–246
54. Ehlert FJ (1988) Estimation of the affinities of allosteric ligand using radioligand binding and pharmacological null methods. Mol Pharmacol 33:187–194
55. Gaddum JH (1937) The quantitative effects of antagonistic drugs. J Physiol 89:7P–9P
56. Doyle DA, Lee A, Lewis J, Kim E, Sheng M, Mackinnon R (1996) Crystal structures of a complexed and peptide-free membrane protein-binding domain—molecular basis of peptide recognition by PDZ. Cell 85:1067–1076
57. Zhou Y, Mackinnon R (2003) The occupancy of ions in the K^+ selectivity filter: charge balance and coupling of ion binding to a protein conformational change underlie high conduction rates. J Mol Biol 333:965–975
58. Kuo A, Gulbis JM, Antcliff JF, Rahman T, Lowe ED, Zimmer J, Cuthbertson J, Ashcroft FM, Ezaki T, Doyle DA (2003) Crystal structure of the potassium channel KirBac1.1 in the closed state. Science 300:1922–1926
59. Capener CE, Proks P, Ashcroft FM, Sansom MSP (2003) Filter flexibility in a mammalian K channel:models and simulations of Kir6.2 mutants. Biophys J 84:2345–2356
60. Friedman R, Nachiel E, Gutman M (2003) The role of intra-protein cavities in the catalytic cycle of bacteriorhodopsin. Biophys J 85:886–896
61. VanDongen AMJ, Chapman ML (2001) K channel gating by an affinity switching selectivity filter. Biophys J 80:16a
62. VanDongen AMJ (2004) K channel gating by an affinity-switching selectivity filter. Proc Natl Acad Sci USA 101:3248–3252
63. Valiyaveetil FI, Sekedat M, Mackinnon R, Muir TW (2004) Glycine as a D-amino acid surrogate in the K-selectivity filter. Proc Natl Acad Sci USA 101:17045–17049
64. Chapman ML, Krovetz HS, VanDongen AMJ (2001) GYGD pore motifs in neighboring potassium channel subunits interact to determine ion selectivity. J Physiol 530:21–33
65. Hurst RS, Toro L, Stefani E (1996) Molecular determinants of external barium block in Shaker potassium channels. FEBS Lett 388:59–65
66. Chen FS, Steele D, Fedida D (1997) Allosteric effects of permeating cations on gating currents during K^+ channel deactivation. J Gen Physiol 110:87–100
67. Capener CE, Shrivastava IH, Ranatunga KM, Forrest LR, Smith GR, Sansom MS (2000) Homology modeling and molecular dynamics simulation studies of an inward rectifier potassium channel. Biophys J 78:2929–2942
68. Consiglio JF, Andalib P, Korn SJ (2003) Influence of pore residues on permeation properties in the Kv2.1 potassium channel. Evidence for a selective functional interaction of K^+ with the outer vestibule. J Gen Physiol 121:111–124
69. Choi KL, Aldrich RW, Yellen G (1991) Tetraethylammonium blockade distinguishes two inactivation mechanisms in voltage-activated K^+ channels. Proc Natl Acad Sci USA 88:5092–5095
70. Starkus JG, Kuschel L, Rayner MD, Heinemann SH (1997) Ion conduction through C-type inactivated Shaker channels. J Gen Physiol 110:539–550
71. Yang Y, Yan Y, Sigworth FJ (1997) How does the W434F mutation block current in Shaker potassium channels? J Gen Physiol 109:779–789
72. Yang Y, Yan Y, Sigworth FJ (1997) How does the W434F mutation block current in Shaker potassium channels? J Gen Physiol 109:779–789
73. Harris RE, Larsson HP, Isacoff EY (1998) A permanent ion binding site located between two gates of the Shaker K^+ channel. Biophys J 74:1808–1820
74. Molina A, Castellano AG, Lopez-Barneo J (1997) Pore mutations in Shaker K^+ channels distinguish between the sites of tetraethylammonium blockade and C-type inactivation. J Physiol 499:361–367
75. Zhou Y, Morais-Cabral JH, Kaufman A, Mackinnon R (2001) Chemistry of ion coordination and hydration revealed by a K^+ channel–Fab complex at 2.0 Å resolution. Nature 414:43–48
76. Woodhull AM (1973) Ionic blockage of sodium channels in nerve. J Gen Physiol 61:687–708
77. Sigworth FJ, Sine SM (1987) Data transformations for improved display and fitting of single channel dwell-time histograms. Biophys J 52:1047–1054